

---

# TRUSTWORTHY AI/ML REGRESSION AND UNBIASED CAUSAL INFERENCE FOR REAL-WORLD DATA

---

Yifei Xu<sup>1,2,3</sup>, Hwiyoung Lee<sup>1,2,3</sup>, Zhenyao Ye<sup>1,2,3</sup>, Yezhi Pan<sup>4</sup>, Jingsong Zhou<sup>4</sup>, Yun Yang<sup>4</sup>,  
Chixiang Chen<sup>1,3</sup>, Shuo Chen<sup>1,2,3,\*</sup>

<sup>1</sup>Division of Biostatistics and Bioinformatics, Department of Epidemiology and Public Health,  
School of Medicine, University of Maryland

<sup>2</sup>Maryland Psychiatric Research Center, Department of Psychiatry,  
School of Medicine, University of Maryland

<sup>3</sup>The University of Maryland Institute for Health Computing (UM-IHC)

<sup>4</sup>Department of Mathematics, University of Maryland, College Park

\*shuochen@som.umaryland.edu

May 26, 2026

## ABSTRACT

Real-World Data (RWD), with its large sample sizes and rich clinical detail, offers a compelling alternative to randomized controlled trials (RCTs) for studying treatment effects in diverse and complex patient populations. However, its observational nature introduces confounding that prevents straightforward comparative effectiveness research. Target trial emulation leverages RWD to estimate average treatment effects (ATE) at the population scale and diversity that RCTs cannot achieve, yet its validity depends critically on unbiased ATE estimation under high-dimensional confounding. Many causal inference pipelines address high-dimensional confounding through machine learning and artificial intelligence (ML/AI) outcome regression. However, commonly used ML/AI regression models exhibit systematic prediction bias, with predicted outcomes shrinking toward the marginal outcome mean. This structural bias propagates into ATE estimation and cannot be corrected by cross-fitting, ensemble methods, or any standard ML practice. In this work, we first quantitatively characterize how systematic prediction bias in ML/AI outcome regression leads to biased ATE estimates in causal inference models. We further propose an unbiased ML/AI regression-based causal inference framework to ensure unbiased ATE estimation for observational studies. We demonstrate our approach by studying the effects of opioids on cardiovascular health in patients with chronic pain using UK Biobank data.

## 1 Introduction

Real-World Data (RWD) is routinely generated from a variety of healthcare sources, including electronic health records (EHRs), administrative claims databases, disease registries, and wearable device monitoring, capturing patient experiences outside the controlled setting of clinical trials. Such data are then used to generate Real-World Evidence (RWE), which helps evaluate the safety and effectiveness of medical products across diverse patient populations [Hubbard et al., 2024, Antoine et al., 2023, Fu et al., 2023, Kuehne et al., 2022]. While randomized clinical trials (RCTs) remain the gold standard for establishing causal treatment effects, their practical limitations are well recognized: they are costly, time-consuming, and their strict eligibility criteria may systematically exclude patients with multiple comorbidities and underrepresented minority populations, precisely the groups bearing the greatest disease burden in routine practice.

Target trial emulation (TTE) provides a principled framework for bridging this gap [Hernán and Robins, 2016]. By explicitly mapping the design features of a hypothetical RCT onto an observational dataset, TTE guards against common

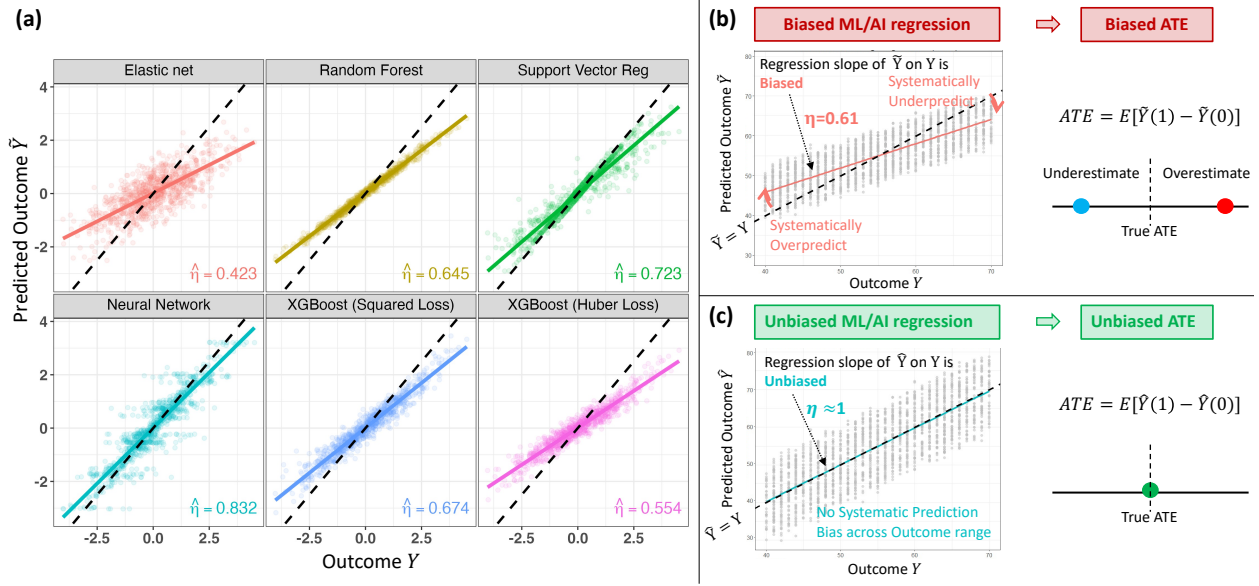


Figure 1: Illustration of systematic prediction bias across ML/AI regression models and its propagation into causal inference. (a) Scatter plots of predicted outcome  $\hat{Y}$  vs. true outcome  $Y$  for representative ML/AI regression models (random forests, XGBoost, neural networks, LASSO, and XGBoost with Huber loss for both training and testing sets). The dashed diagonal is the no-bias reference ( $\hat{Y} = Y$ ); the solid line is the fitted regression with estimated slope  $\hat{\eta}$ . SPB is present whenever  $1 - \hat{\eta} \neq 0$ , i.e., the solid line deviates from the dashed line. This pattern is ubiquitous across all ML regression (MLR) objective functions considered. (b) SPB in the MLR models propagates directly into biased ATE estimation for S-, T-, and X-learners; the magnitude and direction of ATE bias are governed by  $\eta$ . (c) The proposed unbiased ML regression (UMLR) framework achieves  $1 - \hat{\eta} \approx 0$ , yielding unbiased potential-outcome predictions and unbiased ATE estimates.

biases in observational research and enables studies of treatment effects at a scale, duration, and population breadth that no RCT could feasibly achieve. Unbiased estimation of the average treatment effects (ATE) is a fundamental requirement for TTE to yield valid biomedical conclusions that guide clinical practice and inform evidence-based decision making.

In this study, however, we show that ATE estimation for continuous outcomes in TTE can lead to nonnegligible *bias* in the high-dimensional confounding settings common to RWE data when machine learning and artificial intelligence (ML/AI) regression is used to model potential outcomes. The root cause is likely systematic prediction bias (SPB), a widespread yet underappreciated property of ML/AI regression.

**Systematic Prediction Bias in ML/AI regression.** Regression plays a central role in both statistics and machine learning as a standard framework for predicting continuous outcomes. Although AI has achieved remarkable progress in language and categorical tasks, such as text generation and topic classification, regression remains the foundational tool for applications involving continuous outcomes. However, as illustrated in Figure 1 (a), standard ML/AI regression models, including random forests, gradient boosting, kernel methods, deep neural networks, and regularized regression all exhibit a characteristic shrinkage pattern: large outcome values are underpredicted while small outcome values are overpredicted, with predictions uniformly shrinking toward the marginal outcome mean [Lee and Chen, 2025].

This systematic prediction bias emerges because commonly used objective functions such as mean squared error (MSE) favor solutions with bias in exchange for reduced variance, a trade-off that improves overall prediction accuracy but introduces a deterministic, direction-dependent prediction error. While SPB may reduce the MSE and is therefore “acceptable” in pure prediction settings, it is not acceptable when ML/AI regression is used to compute potential outcomes in a causal inference pipeline: the resulting ATE bias is structural and cannot be removed by cross-fitting, sample splitting, ensemble aggregation, or any other standard ML practice, as demonstrated in Figure 1 (b).

**Contributions.** In this article, we propose a novel causal inference framework using *trustworthy* AI/ML regression for RWD-based TTE. Specifically, we:

1. identify a severe and previously unrecognized problem of biased ATE estimation in general AI/ML regression-based causal inference models, driven by the inherent systematic prediction bias in AI/ML regression;
2. derive how the metric of systematic prediction bias in AI/ML regression quantitatively determines the bias of ATE estimation in causal inference models;
3. introduce a new causal inference framework built on unbiased ML regression (UMLR) that yields unbiased ATE estimates;
4. highlight, from a statistical standpoint, the importance of implementing *trustworthy* AI/ML in causal inference, and provide a real-world application to UK Biobank data studying the effect of opioid therapy on blood pressure in patients with chronic pain.

## 2 Methods

### 2.1 Regression Prediction in Causal Inference

RWD datasets routinely record hundreds to thousands of covariates per patient, necessitating flexible ML/AI models within causal inference pipelines. We focus on continuous outcomes, which encompass a broad range of clinically relevant primary endpoints, from blood pressure and cognitive function to disease progression scales [Hubbard et al., 2024]. Under the potential outcome framework [Rubin, 1974], we denote the ATE as  $\Delta = \mathbb{E}[Y(1) - Y(0)]$ , where  $Y$  is a continuous outcome,  $T \in \{0, 1\}$  is a binary treatment indicator,  $X \in \mathbb{R}^p$  represents high-dimensional covariates, and  $Y(t)$  is the potential outcome under treatment  $T = t$ . We observe  $n$  i.i.d. tuples  $\{Y_i, X_i, T_i\}_{i=1}^n$ . The identification of ATE requires several standard assumptions: consistency, the stable unit treatment value assumption (SUTVA), no unmeasured confounding, and positivity [Imbens and Rubin, 2015].

The conditional average treatment effect (CATE) is  $\tau(x) = \mu_1(x) - \mu_0(x)$ , where  $\mu_t(x) = \mathbb{E}[Y \mid T = t, X = x]$ . The ATE is then estimated as

$$\hat{\Delta} = \frac{1}{n} \sum_{i=1}^n [\hat{\mu}_1(X_i) - \hat{\mu}_0(X_i)]. \quad (1)$$

Unbiased prediction of the potential outcome  $\hat{\mu}_t$  yields an ATE estimate approximating the RCT benchmark; however, systematic bias in  $\hat{\mu}_t$  propagates directly into the ATE estimate. We next articulate how systematic bias in ML/AI regression induces biased ATE estimates.

### 2.2 Systematic Prediction Bias (SPB) in ML/AI Regression

**ML/AI regression notation.** Let  $f$  denote an ML/AI predictive function  $f$  that predicts the continuous outcome  $\hat{Y}_i = f(X_i)$  thus providing  $\hat{\mu}_t(X_i)$  for all treatment arms. Without loss of generality, we center the outcome so that  $n^{-1} \sum_{i=1}^n Y_i = 0$ .

**Systematic prediction bias of ML/AI regression.** We consider predicted outcome as unbiased given  $Y$ , if  $\mathbb{E}(\hat{Y}_i \mid Y_i = y^*) = y^*$  for all  $y^*$  in the support of  $Y$  (see Fig 1.c). Throughout the paper, we use  $\hat{Y}$  to denote a generic prediction and  $\tilde{Y}$  to denote the special case of  $\hat{Y}$  that is systematically biased; that is,  $\mathbb{E}(\tilde{Y}_i \mid Y_i = y^*) \neq y^*$ . The prediction bias is systematic if it depends on the true outcome through a deterministic function  $h(\cdot)$ , for example,  $\mathbb{E}(\tilde{Y}_i - Y_i \mid Y_i = y^*) = h(y^*)$ . Systematic prediction bias can be illustrated using scatter plots of  $\hat{Y}$  versus  $Y$  (e.g., Fig 1.b).

As demonstrated in Figure 1(a), SPB is present in all tested ML/AI regression models for both the training and testing datasets [Belitz and Stackelberg, 2021, Zhang and Lu, 2012, Lee and Chen, 2025]. The term “systematic” indicates that the prediction error is not merely random noise, but instead follows a non-random pattern determined by the outcome value itself. Lee and Chen [2025] shows that predicted outcomes exhibiting SPB can reduce empirical loss functions, such as the mean squared error (MSE). Therefore, most regression models tend to favor biased predictions due to the well-known bias-variance tradeoff. SPB is not due to the use of optimization algorithms in ML/AI regression. Instead, it is a universal phenomenon arising from the use of objective functions for continuous outcome like MSE, and is also present in ordinary least squares (OLS) regression. Although OLS yields unbiased parameter estimates and unbiased predictions conditional on predictors,  $\mathbb{E}(\hat{Y} - Y \mid X) = 0$ , the underappreciated fact is that  $\mathbb{E}(\hat{Y} - Y \mid Y) \neq 0$  [Treder et al., 2021].

**A Metric for Characterizing Systematic Prediction Bias.** As the degree of systematic prediction bias varies across  $Y$ , an overall metric is desirable to characterize it over the support of  $Y$ . Based on a large body of literature [Smith et al.,

2019, Butler et al., 2021], the most frequently observed form of  $h(y)$  follows a linear pattern:

$$\mathbb{E}(\tilde{Y}_i - Y_i \mid Y_i = y^*) = h(y^*) - y^* = (\eta - 1)y^*, \quad \eta \in [0, 1]. \quad (2)$$

That is,  $\mathbb{E}(\tilde{Y}_i \mid Y_i = y^*) = \eta y^*$ : every conditional expectation of the predicted outcome is shrunk toward zero (i.e., toward the grand mean of  $Y$  before centering) by a factor of  $\eta$ . Under this linear trend pattern, the bias is most pronounced at the extremes: large outcome values are systematically underpredicted and small outcome values are systematically overpredicted (see Fig 1a). We therefore quantify the degree of SPB by  $1 - \eta$  (or equivalently  $100(1 - \eta)\%$ ), where  $1 - \eta = 0$  indicates no bias. In practice,  $\eta$  can be estimated by the OLS slope  $\hat{\eta}$  obtained from regressing ML/AI regression predicted outcome  $\hat{Y}$  on  $Y$ .

### 2.3 Biased ATE Estimation Induced by Systematic Prediction Bias

Because causal inference pipelines rely on ML/AI regression models to estimate predicted outcomes  $\hat{\mu}_t(X)$  under high-dimensional confounding, the systematic prediction bias of  $\hat{\mu}_t(X)$  propagates directly into ATE estimation. We illustrate this through analytical derivations for several commonly used causal inference models below [Künzel et al., 2019], and further express the resulting ATE bias explicitly in terms of the SPB metric  $\eta$ .

**S-learner.** The S-learner (single learner) fits a single outcome model using the covariates  $X$  and treatment indicator  $T$  jointly to estimate  $\mu_t(X)$ . With bias factor  $\eta_s$ , we have  $\mathbb{E}[\hat{\mu}_t(X)] = \eta_s \mu_t(X)$ , where  $\Delta = \mathbb{E}[\mu_1(X) - \mu_0(X)]$ . It yields

$$\text{Bias}(\hat{\Delta}) = \mathbb{E}[\hat{\Delta}] - \Delta = \mathbb{E}[\eta_s(\mu_1(X) - \mu_0(X))] - \Delta = \eta_s \Delta - \Delta = (\eta_s - 1)\Delta. \quad (3)$$

The bias is linear in  $\eta_s - 1$  and proportional to the true ATE, which simply attenuates  $\Delta$ .

**T-learner.** The T-learner (two learners) fits two separate outcome models in the treated and control groups to estimate  $\mu_1(X)$  and  $\mu_0(X)$ . Suppose the treated and control outcome models exhibit arm-specific bias factors  $\eta_{t1}$  and  $\eta_{t0}$ , respectively, such that  $\mathbb{E}[\hat{\mu}_1(X)] = \eta_{t1}\mu_1(X)$  and  $\mathbb{E}[\hat{\mu}_0(X)] = \eta_{t0}\mu_0(X)$ . Then, we have

$$\text{Bias}(\hat{\Delta}) = \mathbb{E}[(\eta_{t1} - 1)\mu_1(X) - (\eta_{t0} - 1)\mu_0(X)] = (\eta_{t1} - 1)\Delta + (\eta_{t1} - \eta_{t0})\mathbb{E}[\mu_0(X)]. \quad (4)$$

When  $\eta_{t1} \neq \eta_{t0}$ , the bias depends on the absolute level of outcome means, and can reverse the sign of the estimated ATE even when the true effect is large.

**X-learner.** The X-learner (cross learners) extends the T-learner through a two-stage procedure to estimate the CATE [Künzel et al., 2019].

*Stage 1 (Outcome Modeling).* Separate outcome models are fit in the treated and control groups to estimate  $\mu_1(X)$  and  $\mu_0(X)$ . These models are used to construct imputed individual treatment effects (pseudo-outcomes):

$$D^{(1)} = Y - \hat{\mu}_0(X) \quad \text{for treated individuals}, \quad D^{(0)} = \hat{\mu}_1(X) - Y \quad \text{for control individuals}.$$

*Stage 2 (Treatment Effect Modeling).* Two additional models are fit by regressing  $D^{(1)}$  and  $D^{(0)}$  on  $X$ , yielding  $\hat{\tau}_1(X)$  and  $\hat{\tau}_0(X)$ . These estimates are combined using a weighting function  $g(X)$ :

$$\hat{\tau}(X) = g(X)\hat{\tau}_0(X) + \{1 - g(X)\}\hat{\tau}_1(X).$$

We therefore introduce four multiplicative bias factors:  $\eta_{t1}$  and  $\eta_{t0}$  for the treated and control outcome models in the first stage, and  $\eta_{x1}$  and  $\eta_{x0}$  for the second-stage treatment effect models fitted to  $D^{(1)}$  and  $D^{(0)}$ , respectively. The resulting ATE bias is

$$\begin{aligned} \text{Bias}(\hat{\Delta}) = & \mathbb{E}[\{g(X)\eta_{x0}\eta_{t1} + (1 - g(X))\eta_{x1} - 1\} \mu_1(X)] \\ & - \mathbb{E}[\{g(X)\eta_{x0} + (1 - g(X))\eta_{x1}\eta_{t0} - 1\} \mu_0(X)], \end{aligned} \quad (5)$$

where  $g(X)$  is the weighting function. The accumulation of bias across two estimation stages can inflate the variability of the ATE bias.

**Remark.** Due to SPB in existing ML/AI regression models, commonly used causal inference frameworks can yield biased ATE estimates (see the impact of SPB on doubly robust estimator in Appendix.1). Standard correction strategies do not resolve this problem. Cross-fitting cannot address SPB because it arises from the objective function itself; as long as the same MSE objective is used, SPB persists in both the training and test sets [Chernozhukov et al., 2018]. This differs from overfitting, which can often be mitigated through sample splitting. Post-hoc correction strategies are also inadequate: by directly incorporating the observed outcome  $Y$  into the predicted potential outcome  $\hat{\mu}_t(X)$ , they conflate the observed and counterfactual distributions and may fail to account for confounding [Smith et al., 2019, Butler et al., 2021]. *Trustworthy ML/AI* methods that eliminate systematic prediction bias are therefore needed for unbiased ATE estimation.

## 2.4 From Unbiased ML/AI Regression to Unbiased Causal Inference

**Unbiased ML/AI Regression via Constrained Objective Functions.** We adopt the mean-anchoring constrained objective function to eliminate SPB at the model-training stage [Lee and Chen, 2025]. Specifically, we have :

$$\min_f \sum_{i=1}^n \ell(f(X_i), Y_i) + \lambda \Omega(f) \quad \text{s.t.} \quad \sum_{i \in \mathcal{R}_1} (f(X_i) - Y_i) = 0 \quad \text{and} \quad \sum_{i \in \mathcal{R}_2} (f(X_i) - Y_i) = 0, \quad (6)$$

where  $\Omega$  is a regularizer with tuning parameter  $\lambda$ . The two index sets  $\mathcal{R}_1$  and  $\mathcal{R}_2$  are disjoint and complementary, partitioning the sample of  $Y$ , with  $\mathcal{R}_1 \cup \mathcal{R}_2 = \{1, \dots, n\}$ . For example, using the sample mean as the cut-off gives  $\mathcal{R}_1 = \{i : Y_i \leq \bar{Y}\}$  and  $\mathcal{R}_2 = \{i : Y_i > \bar{Y}\}$ . Imposing the two mean-anchoring constraints enforces  $\eta = 1$ , i.e.,  $\mathbb{E}(\tilde{Y}_i | Y_i = y^*) = y^*$  for all  $y^*$ , eliminating SPB across all ML/AI regression model classes, including tree-based algorithms, kernel methods, and regularized regression [Lee and Chen, 2025].

Let  $\hat{\mu}_t^U(X)$  denote the potential outcome estimated by a UMLR model trained under the constrained objective function (6). Then, we define the UMLR based ATE as

$$\hat{\Delta}^U = \frac{1}{n} \sum_{i=1}^n [\hat{\mu}_1^U(X_i) - \hat{\mu}_0^U(X_i)]. \quad (7)$$

**Unbiased ML regression-based Causal Inference Model.** Because SPB is eliminated at the model-fitting stage, yielding  $\eta = 1$  for every ML/AI regression model, the systematic bias terms derived in Section 2.3 vanish exactly. Consequently, the resulting ATE estimator is unbiased regardless of the choice of causal inference model, as established in Theorem 1.

**Theorem 1.** *For each level of treatment  $T = \{0, 1\}$ , the outcome learner  $\hat{\mu}_t^U$  is trained under the constrained objective function (6). Then the UMLR based ATE estimate in (7) is unbiased:  $\mathbb{E}(\hat{\Delta}^U - \Delta) = 0$ .*

## 3 Simulation Studies

We conducted simulation studies to assess the finite-sample performance of ML/AI regression (MLR) and UMLR and to quantify the impact of systematic prediction bias on causal effect estimation.

**Setup.** Covariates  $X \in \mathbb{R}^p$  were generated from a multivariate normal distribution  $X \sim \mathcal{N}(0, \Sigma)$ , where the covariance matrix  $\Sigma$  has entries  $\Sigma_{ij} = \rho^{|i-j|}$  with  $\rho = 0.3$ . Treatment assignment was generated as  $T_i \sim \text{Bernoulli}(e(X_i))$ ,  $e(X_i) = \text{logit}^{-1}(X_i^\top \gamma)$ , where  $\gamma$  has nonzero entries on a subset of covariates, inducing sparsity in the treatment model. The potential outcomes were defined as

$$Y_i(0) = \mu_0(X_i) + \varepsilon_i, \quad Y_i(1) = \mu_1(X_i) + \varepsilon_i,$$

where  $\varepsilon_i \sim \mathcal{N}(0, \sigma^2)$ .

We repeated each experiment over 200 Monte Carlo replications. Three  $(n, p)$  configurations were considered: (500, 200), (500, 500), and (1000, 200). We further generated data under varying levels of SPB by retaining datasets yielding  $\eta$  approximating target values. We implement S-, T-, and X-learners using both MLR and the proposed UMLR as outcome models. We evaluated estimator performance across different methods, using the RCT estimator as a gold-standard benchmark. For each scenario, we assessed the bias, standard deviation, and coverage probability of the estimated ATE across varying degrees of shrinkage.

**Results: Relationship between  $\eta$  and ATE bias.** Figure 2(a) presents the ATE bias as a function of  $\eta_s$  based on (7). The bias exhibits a linear relationship with  $\eta_s - 1$ , with slope equal to the true ATE  $\Delta = 3$ , consistent with the theoretical result in (3).  $\eta_s < 1$  induces systematic underestimation of the treatment effect, with the magnitude of bias increasing as  $\eta_s \rightarrow 0$ . Conversely, when  $\eta_s = 1$ , the bias vanishes exactly.

Under  $\eta_s = \eta_{t1} = \eta_{t0} = \eta_{x1} = \eta_{x0} \doteq 0.6$ , systematic prediction bias directly translates into negative ATE bias across all MLR-based learners (Figure 2(b)). The S-learner exhibits systematic underestimation of the ATE, as predicted by equation (3). The T-learner yields comparable bias, as uniform shrinkage applied symmetrically to both treatment arms largely cancels in the difference, resulting in an equivalent underestimation as the S-Learner. The X-learner exhibits the largest bias among the three learners, as its multi-stage estimation propagates and accumulates shrinkage errors rather than attenuating them. In contrast, UMLR produces approximately unbiased estimates across learners, closely aligned with the RCT benchmark.

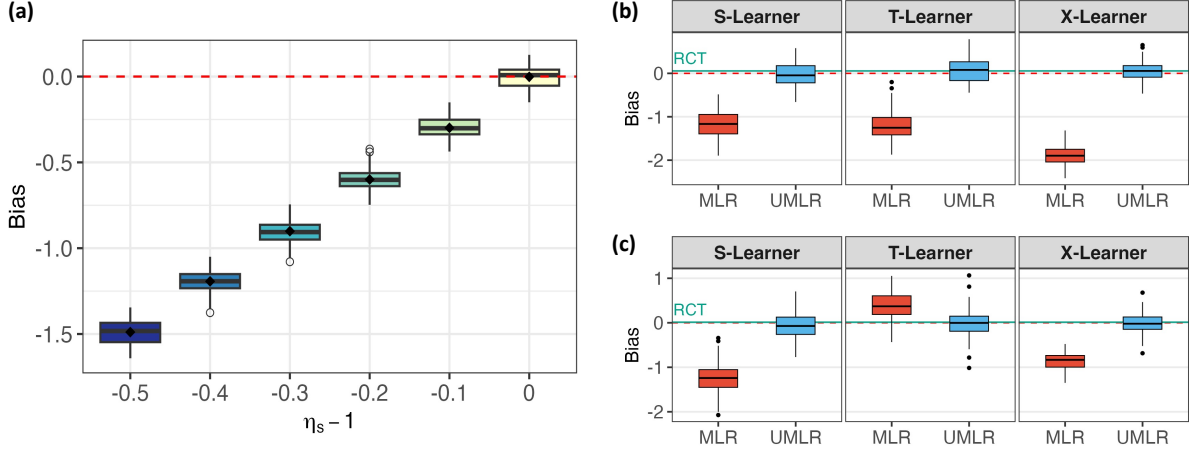


Figure 2: Systematic bias in estimated ATE: **(a)** across data sets with different  $\eta$  values we assess the relationship between bias of ATE and  $\eta_s - 1$ , which further verifies how  $\eta$  impacts bias. **(b)** we focus on datasets with specified SPB of  $\eta_s = \eta_{t1} = \eta_{t0} = \eta_{x1} = \eta_{x0} = 0.6$  and show corresponding bias in ATE estimation **(c)** heterogeneous SPB levels  $\eta_s = 0.6, \eta_{t1} = 0.8, \eta_{t0} = 0.6, \eta_{x1} = 0.8, \eta_{x0} = 0.6$  lead to different biases in ATE. Across all settings, trustworthy AI/ML regression (i.e., UMLR) yields unbiased estimates of ATE.

Under  $\eta_s \doteq 0.6, \eta_{t1} \doteq 0.8, \eta_{t0} \doteq 0.6, \eta_{x1} \doteq 0.8, \eta_{x0} \doteq 0.6$ , shrinkage is no longer symmetric between groups. Figure 2(c) shows that the MLR-based T-learner overestimates the ATE in this setting. The bias is now determined by the difference in group-specific shrinkage, such that  $\eta_{t1} > \eta_{t0}$  reverses the direction of bias, and differential shrinkage between the treated and control outcome models introduces additional distortion beyond the uniform case (see (4)). The MLR-based X-learner exhibits the smallest bias in this setting, yet its multi-stage construction offers no reliable protection, as heterogeneous shrinkage propagates unpredictably across groups and stages and the direction of bias remains difficult to anticipate. (see (5)). UMLR remains approximately unbiased and closely aligned with the RCT benchmark in this scenario.

Table 1 summarizes performance across varying sample sizes  $n$  and dimensionality  $p$ . Overall, UMLR outperforms MLR across the S-, T-, and X-learners for all settings, achieving smaller bias and better coverage. However, this improvement comes at the cost of increased variance.

Table 1: Simulation results comparing the performance of MLR- and UMLR- based meta-learners under SPB.

Method	$\eta$	$n=500, p=200$			$n=500, p=500$			$n=1,000, p=200$		
		Bias (%)	SD	Cov.	Bias (%)	SD	Cov.	Bias (%)	SD	Cov.
<i>S-learner</i>										
MLR	0.6	39.80	0.28	0.01	40.60	0.33	0.04	40.13	0.21	0.00
UMLR	—	0.10	0.35	0.97	0.44	0.32	0.96	0.29	0.20	0.94
<i>T-learner</i>										
MLR	(0.6, 0.6)	40.16	0.30	0.02	40.62	0.33	0.04	39.52	0.22	0.00
MLR	(0.8, 0.6)	13.43	0.30	0.72	14.07	0.32	0.71	13.10	0.25	0.62
UMLR	—	0.06	0.29	0.97	0.55	0.32	0.93	1.23	0.21	0.94
<i>X-learner</i>										
MLR	(0.6, 0.6, 0.6, 0.6)	62.38	0.19	0.00	78.61	0.19	0.00	63.09	0.13	0.00
MLR	(0.8, 0.6, 0.8, 0.6)	29.43	0.20	0.01	44.01	0.22	0.00	29.32	0.13	0.00
UMLR	—	1.60	0.31	0.97	0.34	0.34	0.97	0.10	0.22	0.96

Bias(%): mean absolute bias as % of true ATE; Cov.: empirical 95% CI coverage.

## 4 RWD Application: Opioid Therapy and Blood Pressure in Chronic Pain

We applied the proposed framework to estimate the ATE of opioid use on systolic blood pressure among participants with chronic pain using UK Biobank data. Chronic pain was defined as self-reported pain lasting more than three months in any of seven body regions (headaches, facial pain, neck/shoulder, back, stomach/abdominal, hip, and knee) at baseline. Opioid use was determined from self-reported current medications at the imaging visit, classified using Anatomical Therapeutic Chemical (ATC) codes [Gao et al., 2024]. The primary outcome was the mean of two systolic blood pressure measurements at the imaging visit, with fewer than two measurements treated as missing. The final analytic sample comprised 19,736 participants with chronic pain, of whom 523 were opioid users and 19,213 were non-users. Covariates included age, sex, baseline blood biomarkers and others, yielding  $p = 35$  variables in total (see Appendix Table 2). The ATE was estimated using MLR and UMLR incorporated into S-, T-, and X-learners. Propensity score matching (PSM) was also applied as a benchmark, because it does not rely on ML/AI regression-predicted outcomes and is therefore not affected by SPB [Rosenbaum and Rubin, 1983]. Following matching, confounding variables were well balanced between the two treatment arms (see Appendix A.4), and therefore the average treatment effect on the treated (ATT) estimated by PSM was used as the reference, while noting that the ATT estimand differs from the ATE and the sample size for PSM is smaller.

As demonstrated in Figure 3(a), both UMLR-based and conventional MLR-based causal inference models indicate that opioid treatment for pain management significantly reduces systolic blood pressure relative to no medication (all  $p < 0.001$ ), consistent with previous studies [Sacco et al., 2013, Qin et al., 2026]. However, the estimated ATEs differ substantially: UMLR-based estimators yield larger negative estimates of  $-4.72$ ,  $-4.94$ , and  $-5.29$  mmHg for the S-, T-, and X-learners, respectively, closely aligned with the PSM benchmark of  $-5.08$  mmHg, whereas MLR-based estimators produce substantially attenuated estimates of  $-2.41$ ,  $-3.83$ , and  $-2.36$  mmHg. This attenuation is consistent with the SPB-induced bias characterized in Section 2.3. As shown in Figure 3(b), conventional MLR exhibits substantial SPB, with  $\hat{\eta}_S = 0.409$  and  $\hat{\eta}_T = 0.410$  on the training set, and  $\hat{\eta}_S = 0.148$  and  $\hat{\eta}_T = 0.147$  on the test set. In contrast, UMLR achieves near-zero SPB, with  $\hat{\eta}_S = 0.922$  and  $\hat{\eta}_T = 0.923$  on the training set, and  $\hat{\eta}_S = 0.903$  and  $\hat{\eta}_T = 0.904$  on the test set. The discrepancy in ATE estimates between MLR- and UMLR-based causal inference models is therefore likely driven by SPB-induced bias.

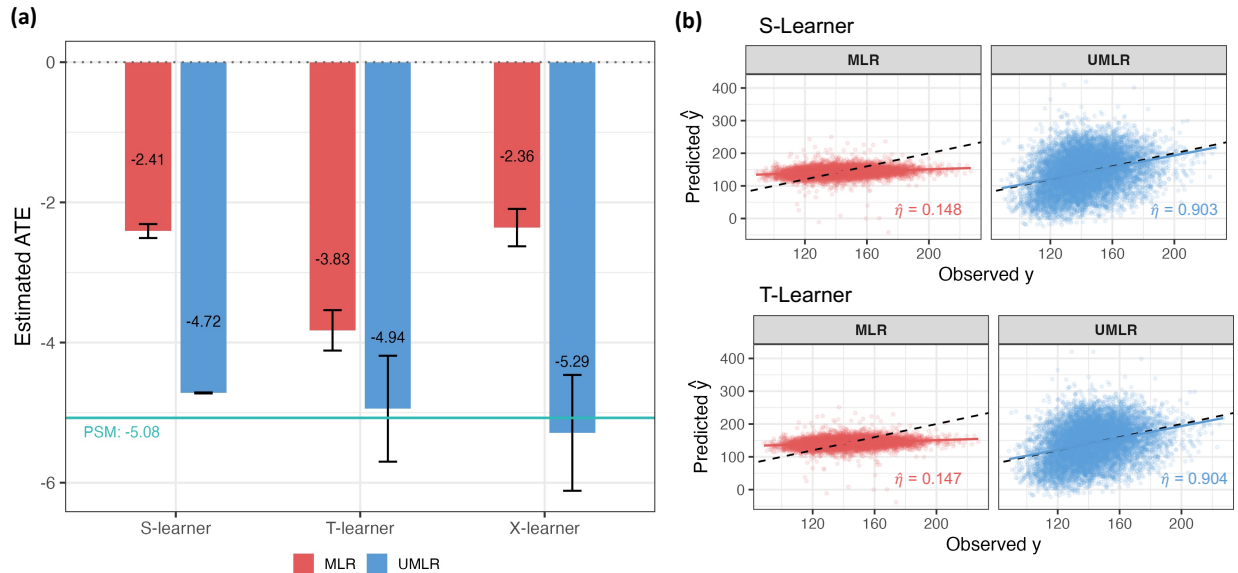


Figure 3: Results of real data application on mean systolic blood pressure under opioid treatment vs. no-medication. (a) ATE estimates with 95% confidence intervals (b) Predicted vs. observed systolic blood pressure for the S-learner and T-Learner under MLR and UMLR for the testing datasets. The dashed line denotes the prediction without systematic bias. (i.e.,  $\eta = 1$ ).

## 5 Discussion

Despite the advancement in ML/AI, a structural vulnerability still remains in current ML/AI regression tasks and its application in RWE-based TTE analysis: systematic prediction bias, widely seen in standard ML/AI regression algorithms, propagates into biased ATE estimates for regression-based causal machine learning methods in ways that may not be corrected by cross-fitting, ensemble methods, or model selection. We have proposed a principled remedy in the form of UMLR, which mitigate SPB at the model-fitting stage. It has been shown that the resulting causal inference framework built on UMLR yields unbiased ATE estimates.

Notably, outcome regression-based causal inference models are attractive in many applications. Compared with weighing-based approaches, outcome regression-based causal inference models can be less sensitive to instability arising from extreme weights, which may occur in settings with limited overlap (as in our UKB data application). In many practical scenarios, this can translate into improved finite-sample performance, including MSE, particularly when the outcome model is reasonably well-specified. Outcome regression-based models are especially convenient in settings with continuous treatments or exposures, where direct modeling of the outcome surface can be more straightforward than constructing and stabilizing generalized propensity scores.

Based on these findings, we recommend: i) routinely diagnosing and reporting SPB via  $1 - \hat{\eta}$  for all potential outcome models, including both ML/AI regression and OLS; and ii) adopting UMLR-based causal inference for unbiased ATE estimation in RWE-based TTE. The main limitations are a modest increase in prediction variance relative to unconstrained ML regression, as the cost of mitigating structural bias, and a currently limited set of implemented UMLR models, both of which will be addressed in future work.

## Data and Code Availability

This research was conducted using the UK Biobank Resource under application number 74376. The code used for analyses is available on GitHub at <https://github.com/effyifeixu/Unbiased-Causal>.

## Acknowledgement

The authors thank the UK Biobank for their efforts in data collection and curation, which made this research possible.

## References

- A. Antoine et al. Target trial emulation to assess real-world efficacy in the treatment of metastatic breast cancer. *Journal of the National Cancer Institute*, 115(8):971–980, 2023.
- K. Belitz and P.E. Stackelberg. Evaluation of six methods for correcting bias in estimates from ensemble tree machine learning regression models. *Environmental Modelling & Software*, 139:105006, 2021. ISSN 1364-8152. doi: <https://doi.org/10.1016/j.envsoft.2021.105006>. URL <https://www.sciencedirect.com/science/article/pii/S1364815221000499>.
- Ellyn R. Butler, Andrew Chen, Rabie Ramadan, Trang T. Le, Kosha Ruparel, Tyler M. Moore, Theodore D. Satterthwaite, Fengqing Zhang, Haochang Shou, Ruben C. Gur, Thomas E. Nichols, and Russell T. Shinohara. Pitfalls in brain age analyses. *Human Brain Mapping*, 42(13):4092–4101, 2021. doi: <https://doi.org/10.1002/hbm.25533>. URL <https://onlinelibrary.wiley.com/doi/abs/10.1002/hbm.25533>.
- Victor Chernozhukov, Denis Chetverikov, Mert Demirer, Esther Duflo, Christian Hansen, Whitney Newey, and James Robins. Double/debiased machine learning for treatment and structural parameters. *The Econometrics Journal*, 21(1):C1–C68, 2018.
- E. L. Fu et al. Target trial emulation to improve causal inference from observational data: What, why, and how? *Journal of the American Society of Nephrology*, 2023.
- Yaqing Gao, Binbin Su, Lei Ding, Danial Qureshi, Shenda Hong, Jie Wei, Chao Zeng, Guanghua Lei, and Junqing Xie. Association of regular opioid use with incident dementia and neuroimaging markers of brain health in chronic pain patients: analysis of uk biobank. *The American Journal of Geriatric Psychiatry*, 32(9):1154–1165, 2024.
- Miguel A Hernán and James M Robins. Using big data to emulate a target trial when a randomized trial is not available. *American Journal of Epidemiology*, 183(8):758–764, 2016.
- Rebecca A. Hubbard et al. Target trial emulation for observational studies. *New England Journal of Medicine*, 2024. doi: 10.1056/NEJMp2407586.

- Guido W Imbens and Donald B Rubin. Causal inference in statistics, social, and biomedical sciences. Cambridge university press, 2015.
- Fabian Kuehne et al. Causal analyses with target trial emulation for real-world evidence removed large self-inflicted biases: Systematic bias assessment of ovarian cancer treatment effectiveness. Journal of Clinical Epidemiology, 152: 269–280, 2022. doi: 10.1016/j.jclinepi.2022.10.005.
- Sören R. Künzel, Jasjeet S. Sekhon, Peter J. Bickel, and Bin Yu. Metalearners for estimating heterogeneous treatment effects using machine learning. Proceedings of the National Academy of Sciences, 116(10):4156–4165, 2019. doi: 10.1073/pnas.1804597116.
- Hwiyoung Lee and Shuo Chen. Systematic bias of machine learning regression models and correction. IEEE Transactions on Pattern Analysis & Machine Intelligence, 47(06):4974–4983, 2025.
- Fan Li, Laine E. Thomas, and Fan Li. Addressing extreme propensity scores via the overlap weights. American Journal of Epidemiology, 188(1):250–257, 2019. doi: 10.1093/aje/kwy201.
- Pei Qin, Frederick K Ho, Carlos A Celis-Morales, and Jill P Pell. Chronic pain and hypertension and mediation role of inflammation and depression. Hypertension, 83(1):146–156, 2026.
- Jeremy A. Rassen et al. High-dimensional propensity scores for empirical covariate selection in secondary database studies: Planning, implementation, and reporting. Pharmacoepidemiology and Drug Safety, 31(1):73–82, 2022. doi: 10.1002/pds.5372.
- James M Robins, Andrea Rotnitzky, and Lue Ping Zhao. Estimation of regression coefficients when some regressors are not always observed. Journal of the American Statistical Association, 89(427):846–866, 1994.
- Paul R Rosenbaum and Donald B Rubin. The central role of the propensity score in observational studies for causal effects. Biometrika, 70(1):41–55, 1983.
- Donald B Rubin. Estimating causal effects of treatments in randomized and nonrandomized studies. Journal of Educational Psychology, 66(5):688–701, 1974.
- Marcella Sacco, Michele Meschi, Giuseppe Regolisti, Simona Detrenis, Laura Bianchi, Marcello Bertorelli, Sarah Pioli, Andrea Magnano, Francesca Spagnoli, Pasquale Gianluca Giuri, et al. The relationship between blood pressure and pain. The journal of clinical hypertension, 15(8):600–605, 2013.
- Sebastian Schneeweiss, Jeremy A. Rassen, Robert J. Glynn, Jerry Avorn, Helen Mogun, and M. Alan Brookhart. High-dimensional propensity score adjustment in studies of treatment effects using health care claims data. Epidemiology, 20(4):512–522, 2009. doi: 10.1097/EDE.0b013e3181a663cc.
- Stephen M. Smith, Diego Vidaurre, Fidel Alfaro-Almagro, Thomas E. Nichols, and Karla L. Miller. Estimation of brain age delta from brain imaging. NeuroImage, 200:528–539, 2019. ISSN 1053-8119. doi: <https://doi.org/10.1016/j.neuroimage.2019.06.017>. URL <https://www.sciencedirect.com/science/article/pii/S1053811919305026>.
- Matthias S. Treder, Jonathan P. Shock, Dan J. Stein, Stéfan du Plessis, Soraya Seedat, and Kamen A. Tsvetanov. Correlation constraints for regression models: Controlling bias in brain age prediction. Frontiers in Psychiatry, 12, 2021. ISSN 1664-0640. doi: 10.3389/fpsy.2021.615754. URL <https://www.frontiersin.org/journals/psychiatry/articles/10.3389/fpsy.2021.615754>.
- Mark J van der Laan and Daniel Rubin. Targeted maximum likelihood learning. The International Journal of Biostatistics, 2(1):1–38, 2006.
- Guoyi Zhang and Yan Lu. Bias-corrected random forests in regression. Journal of Applied Statistics, 39(1):151–160, 2012. doi: 10.1080/02664763.2011.578621. URL <https://doi.org/10.1080/02664763.2011.578621>.
- Yunji Zhou, Roland A. Matsouaka, and Laine E. Thomas. Propensity score weighting under limited overlap and model misspecification. Statistical Methods in Medical Research, 29(12):3721–3756, 2020. doi: 10.1177/0962280220940334.

## Appendix

### A.1: The Impact of Systematic Prediction Bias on Doubly Robust Estimator

Doubly robust estimators are powerful tools for causal inference because they can provide unbiased estimates when either the propensity score model or the outcome regression model is correctly specified. However, in settings with high-dimensional confounding, the outcome regression component is often modeled using AI/ML regression, which incurs systematic prediction bias [Lee and Chen, 2025]. In this case, the doubly robust estimator loses one layer of

protection and must rely entirely on correct specification of the propensity score model. This reliance can be problematic because propensity score models are known to face several challenges in practice, including instability, limited overlap, and difficulty in accurately modeling treatment assignment under high-dimensional confounding [Schneeweiss et al., 2009, Li et al., 2019, Zhou et al., 2020, Rassen et al., 2022]. Together, these issues can lead to biased ATE estimation.

In the following simulation examples, we show that: (i) the ATE estimate can be biased in many practical settings; (ii) finite-sample bias can persist even when the true propensity score is used in the inverse probability weighting component of a doubly robust estimator, although it gradually shrinks toward zero as the sample size increases; and (iii) modern implementations based on Double Machine Learning (DML) and Targeted Maximum Likelihood Estimation (TMLE) are subject to the same phenomenon. Since such very large sample sizes are often unavailable in real-world applications, trustworthy AI/ML regression remains important for doubly robust causal inference in RWD analysis.

## A.2 Simulation Study: Finite-Sample Bias in Doubly Robust Estimation

We conducted additional simulation studies to evaluate the finite-sample performance of doubly robust estimators when conventional MLR is employed as the outcome regression models for potential outcome prediction with SPB. Specifically, we assess the influence of systematic prediction bias on ATE estimation bias. In addition, we examined the performance of doubly robust model implemented by the double machine learning (DML) estimator [Chernozhukov et al., 2018], and the targeted maximum likelihood estimator (TMLE) [van der Laan and Rubin, 2006].

Using the data-generating procedure of Section 3, we simulated datasets with  $p = 200$  covariates,  $\mu_1 = 8$ ,  $\mu_0 = 5$  ( $\Delta = 3$ ), across sample sizes  $n \in \{100, 500, 2,000, 5,000\}$ .

**The Influence of Systematic Prediction Bias on ATE Estimation in Doubly Robust Estimators.** To attribute bias in doubly robust ATE estimates solely to systematic prediction bias in the outcome model, we use the true propensity score, rather than an ML-estimated counterpart, as the oracle treatment assignment probability. Since doubly robust ATE bias vanishes asymptotically, we evaluate finite-sample bias across  $n \in \{100, 500, 2,000, 5,000\}$ , where  $n = 5,000$  represents a practically large sample. We further consider two noise levels,  $\sigma = 5$  and  $\sigma = 1$ .

As shown in Figure 4(a), doubly robust ATE bias decreases monotonically with sample size, yet convergence to zero is slow: non-negligible bias remains even at  $n = 5,000$ . Counterintuitively, higher noise levels reduce bias. A possible explanation is that elevated noise attenuates the contribution of the outcome regression component to the doubly robust estimator, thereby dampening the influence of systematic prediction bias on ATE estimation. This pattern underscores that conventional MLR-based doubly robust estimators are most sensitive to SPB in high signal-to-noise settings, the very conditions under which precise treatment effect estimates are most consequential for clinical decision-making.

**Bias of ATE Estimation Across Doubly Robust Estimators.** To examine whether the influence of systematic prediction bias on ATE estimation generalizes beyond AIPW, we additionally evaluated DML and TMLE at  $n = 500$ . As shown in Figure 4(b), non-negligible ATE bias persists across all three doubly robust estimators, indicating that systematic prediction bias is a framework-level phenomenon not attributable to any particular estimator. These results suggest that UMLR provides a broadly applicable correction strategy for potential outcome prediction, offering consistent bias reduction across the doubly robust estimator family.

## A.3 Unbiased ATE by UMLR-based Causal Inference Models

### A.3.1 Proof of Theorem 1

The two constraints in (6) imply

$$\sum_{i \in \mathcal{R}_1} (f^*(X_i) - Y_i) = 0 \quad \text{and} \quad \sum_{i \in \mathcal{R}_2} (f^*(X_i) - Y_i) = 0.$$

Adding these two equations gives

$$\begin{aligned} 0 &= \sum_{i \in \mathcal{R}_1} (f^*(X_i) - Y_i) + \sum_{i \in \mathcal{R}_2} (f^*(X_i) - Y_i) \\ &= \sum_{i \in \mathcal{R}_1} (\hat{f}(X_i) - c\tilde{f}(X_i) - Y_i) + \sum_{i \in \mathcal{R}_2} (\hat{f}(X_i) - c\tilde{f}(X_i) - Y_i) \\ &= \sum_{i=1}^n (\hat{f}(X_i) - Y_i) - c \sum_{i=1}^n \tilde{f}(X_i), \end{aligned} \tag{8}$$

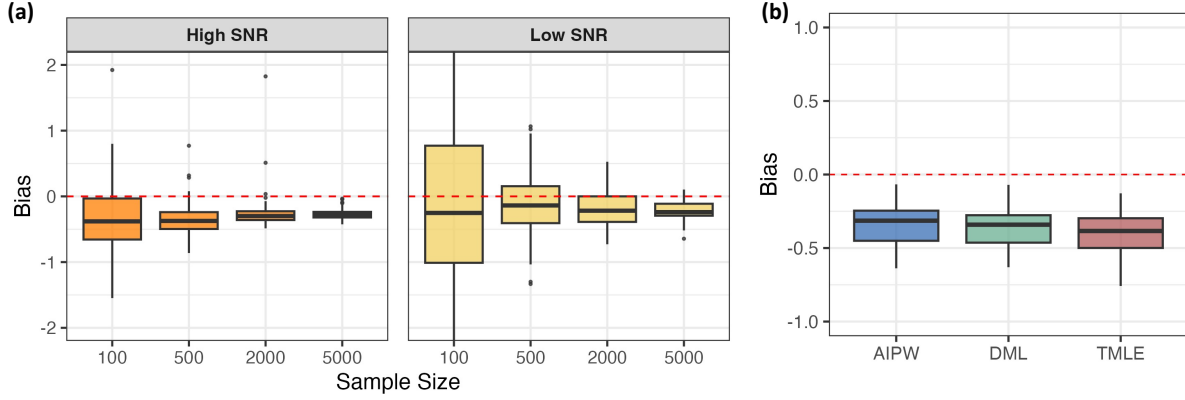


Figure 4: Influence of systematic prediction bias on doubly robust ATE estimation. (a) With oracle propensity scores, ATE bias decreases monotonically with sample size but converges slowly; non-negligible bias remains at  $n = 5,000$ . Higher noise levels attenuate SPB-induced bias in the outcome regression. (b) ATE bias persists across all three doubly robust estimators, AIPW, DML, and TMLE, at  $n = 500$ .

where the second equality substitutes the assumed form  $f^*(X_i) = \mathring{f}(X_i) - c\tilde{f}(X_i)$ , with  $\mathring{f}(X_i)$  an unbiased prediction of  $Y_i$  and  $c$  the systematic bias constant.

Since  $\mathring{f}(X_i)$  is an unbiased prediction of  $Y_i$ , taking the expectation of the first term in (8) gives

$$\mathbb{E}\left[\sum_{i=1}^n (\mathring{f}(X_i) - Y_i)\right] = 0.$$

Taking the expectation of (8) therefore yields

$$0 = 0 - c\mathbb{E}\left[\sum_{i=1}^n \tilde{f}(X_i)\right].$$

To ensure  $c\mathbb{E}\left[\sum_{i=1}^n \tilde{f}(X_i)\right] = 0$  holds for all cases of  $\sum_{i=1}^n f^*(X_i)$ , the constant  $c$  must be 0.

It follows that  $f^*(X_i) = \mathring{f}(X_i)$ , so the predicted potential outcomes satisfy

$$\mathbb{E}[f^*(X_i) | X_i] = \mu_t(X_i), \quad t \in \{0, 1\},$$

where  $\mu_t(X_i) = \mathbb{E}[Y_i(t) | X_i]$  is the true potential outcome mean under arm  $t$ . The ATE estimator constructed from  $f^*$  thus satisfies:

$$\begin{aligned} \mathbb{E}\left[\widehat{\Delta}^{\text{UMLR}}\right] &= \mathbb{E}\left[\frac{1}{n}\sum_{i=1}^n (f^*(X_i^{(1)}) - f^*(X_i^{(0)}))\right] \\ &= \frac{1}{n}\sum_{i=1}^n \mathbb{E}[f^*(X_i^{(1)}) - f^*(X_i^{(0)})] \\ &= \frac{1}{n}\sum_{i=1}^n (\mu_1(X_i) - \mu_0(X_i)) \\ &= \mathbb{E}[\mu_1(X) - \mu_0(X)] \\ &= \Delta. \end{aligned}$$

Therefore, the ATE estimator constructed from the predicted potential outcomes  $f^*$  is unbiased. We also show that the unbiased estimation extends to other causal inference models as follows.

**Unbiased T-learner.** Under UMLR, two separate constrained models are fit, one per treatment arm. Each achieves  $\eta_{t1} = \eta_{t0} = 1$ , so equation (4) gives

$$\text{Bias}\left(\widehat{\Delta}^{\text{T-UMLR}}\right) = (\eta_{t1} - 1) \mathbb{E}[\mu_1(X)] - (\eta_{t0} - 1) \mathbb{E}[\mu_0(X)] = 0. \quad (9)$$

Crucially, because both arm-specific shrinkage factors are eliminated simultaneously, the outcome-level term  $(\eta_{t1} - \eta_{t0})\mathbb{E}[\mu_0(X)]$  that can reverse the sign of the ATE under conventional MLR also vanishes.

**Unbiased X-learner.** The X-learner involves four shrinkage factors across two estimation stages. Under UMLR, all four constrained models satisfy  $\eta_{t1} = \eta_{t0} = \eta_{x1} = \eta_{x0} = 1$ . Substituting into (5),

$$\begin{aligned} \text{Bias}\left(\widehat{\Delta}^{\text{X-UMLR}}\right) &= \mathbb{E}\left[(g(X) \cdot 1 \cdot 1 + (1 - g(X)) \cdot 1 - 1) \mu_1(X)\right] \\ &\quad - \mathbb{E}\left[(g(X) \cdot 1 + (1 - g(X)) \cdot 1 \cdot 1 - 1) \mu_0(X)\right] \\ &= \mathbb{E}\left[(1 - 1) \mu_1(X)\right] - \mathbb{E}\left[(1 - 1) \mu_0(X)\right] = 0. \end{aligned} \quad (10)$$

The multi-stage bias amplification that makes the X-learner especially sensitive to SPB under conventional MLR is thus fully neutralized.

**Unbiased doubly robust estimator.** Under UMLR, both the outcome regression  $\hat{\mu}_t^{\text{U}}$  and the propensity score  $e^{\text{U}}$  are estimated under constrained objectives that enforce  $\eta = 1$ . Substituting unbiased nuisance estimates into the AIPW estimator,

$$\begin{aligned} \mathbb{E}\left[\widehat{\Delta}^{\text{DR-UMLR}}\right] &= \mathbb{E}\left[\hat{\mu}_1^{\text{U}}(X) - \hat{\mu}_0^{\text{U}}(X) + \frac{T}{e(X)}(Y - \hat{\mu}_1^{\text{U}}(X)) - \frac{1 - T}{1 - e(X)}(Y - \hat{\mu}_0^{\text{U}}(X))\right] \\ &= \mathbb{E}[Y(1)] - \mathbb{E}[Y(0)] = \Delta, \end{aligned} \quad (11)$$

where the last equality follows from unconfoundedness and the consistency of  $\hat{\mu}_t^{\text{U}}$  [Robins et al., 1994]. Because the outcome regression is now genuinely unbiased, the double robustness guarantee is fully restored: the estimator remains consistent even under moderate misspecification of the propensity score model, and it achieves semiparametric efficiency when both nuisance functions are correctly specified. ■

**Bias–variance trade-off.** Imposing the constraints in (6) reduces bias at the cost of potentially increased estimator variance, since the feasible set is smaller than that of the unconstrained problem. In finite samples this may raise the MSE of  $f^*$  relative to the unconstrained solution. However, because the ATE estimator is a population-level average of  $f^*(X)$ , the variance inflation is  $O(n^{-1/2})$  and vanishes as  $n \rightarrow \infty$ , whereas the bias of the unconstrained estimator is  $O(1)$  and does not diminish. The constrained solution therefore dominates for the inferential task of ATE estimation whenever  $n$  is moderately large.

### A.3.2 Supplementary Results and Evaluation Metrics

Appendix Table 2 summarizes baseline covariates for participants with chronic pain in the UK Biobank, stratified by opioid use status. The analytic cohort included 19,736 participants, of whom 523 (2.6%) reported current opioid use and 19,213 (97.4%) were non-users, indicating substantial imbalance in treatment group sizes. Compared with non-users, opioid users were older, had higher body mass index, greater socioeconomic deprivation, lower educational attainment, and were more likely to be current or former smokers. They also exhibited less favorable inflammatory and metabolic biomarker profiles, including higher levels of C-reactive protein, glucose, HbA1c, triglycerides, and cystatin C, and lower levels of HDL cholesterol, IGF-1, SHBG, and vitamin D. The substantial differences in baseline characteristics highlight the needs of for careful confounding adjustment when estimating the causal effect of opioid use on blood pressure.

After propensity score matching, 518 opioid users were successfully matched to 518 non-users. Baseline covariates were well balanced between the two groups, with insignificant  $p$ -values and minimal standardized mean differences (generally below 0.1) for all covariates (Appendix Table 3).

Appendix Table 4 evaluates the performance for MLR and UMLR under the S- and T-learners in the UK Biobank chronic pain cohort. Consistent with the simulation results, MLR exhibited noticeable systematic prediction bias, with bias slopes of approximately 0.85 for both learners and strong correlations between observed and prediction residuals ( $\text{Cor}(y, \hat{\varepsilon}) \approx -0.79$ ). In contrast, UMLR substantially reduced prediction bias, with slopes close to zero and near-zero residual correlations, indicating effective removal of systematic prediction bias. UMLR produced larger RMSE and MAE than MLR for both learners. Corresponding diagnostics are not reported for the X-learner because its second-stage models target pseudo-outcomes rather than the observed outcome directly.

Table 2: Descriptive statistics of covariates stratified by opioid use status among participants with chronic pain in the UK Biobank.

Characteristic	Non-users (n = 19,213)	Opioid users (n = 523)	p-value
<i>Demographic and lifestyle characteristics</i>			
Sex = male, %	8384 (43.6)	218 (41.7)	0.398
Age, mean (SD)	53.57 (7.28)	56.53 (7.53)	<0.001
Ethnicity, %			0.797
1 (White)	18482 (96.2)	509 (97.3)	
2 (Mixed)	124 (0.6)	3 (0.6)	
3 (Asian or Asian British)	261 (1.4)	6 (1.1)	
4 (Black or Black British)	150 (0.8)	2 (0.4)	
5 (Chinese)	53 (0.3)	1 (0.2)	
6 (Other ethnic group)	143 (0.7)	2 (0.4)	
Education, %			<0.001
1 (College or University degree)	9244 (48.1)	181 (34.6)	
2 (A levels/AS levels or equivalent)	2798 (14.6)	72 (13.8)	
3 (O levels/GCSEs or equivalent)	4199 (21.9)	157 (30.0)	
4 (CSEs or equivalent)	977 (5.1)	35 (6.7)	
5 (NVQ or HND or HNC or equivalent)	1068 (5.6)	43 (8.2)	
6 (Other professional qualifications eg: nursing, teaching)	927 (4.8)	35 (6.7)	
Smoking status, %			<0.001
0 (Never)	11336 (59.0)	259 (49.5)	
1 (Previous)	6499 (33.8)	210 (40.2)	
2 (Current)	1378 (7.2)	54 (10.3)	
Alcohol drinking status, %			<0.001
0 (Never)	532 (2.8)	17 (3.3)	
1 (Previous)	493 (2.6)	31 (5.9)	
2 (Current)	18188 (94.7)	475 (90.8)	
<i>Anthropometric and socioeconomic measures</i>			
BMI, mean (SD)	26.60 (4.34)	29.65 (5.71)	<0.001
Townsend Deprivation Index, mean (SD)	-1.83 (2.76)	-1.12 (2.98)	<0.001
<i>Blood biomarkers</i>			
Albumin, mean (SD)	45.44 (2.44)	44.94 (2.44)	<0.001
Alkaline phosphatase, mean (SD)	78.99 (22.75)	83.21 (24.30)	<0.001
Alanine aminotransferase, mean (SD)	22.56 (13.16)	24.76 (13.50)	<0.001
Apolipoprotein A, mean (SD)	1.55 (0.25)	1.49 (0.25)	<0.001
Apolipoprotein B, mean (SD)	1.03 (0.22)	1.04 (0.23)	0.494
Aspartate aminotransferase, mean (SD)	25.28 (8.65)	26.10 (9.01)	0.034
Direct bilirubin, mean (SD)	1.73 (0.74)	1.58 (0.59)	<0.001
Urea, mean (SD)	5.22 (1.19)	5.47 (1.32)	<0.001
Calcium, mean (SD)	2.38 (0.09)	2.37 (0.09)	0.100
Cholesterol, mean (SD)	5.71 (1.03)	5.59 (1.13)	0.008
Creatinine, mean (SD)	71.39 (15.09)	70.81 (14.15)	0.384
C-reactive protein, mean (SD)	2.04 (3.47)	3.39 (4.62)	<0.001
Cystatin C, mean (SD)	0.86 (0.13)	0.91 (0.14)	<0.001
Gamma glutamyltransferase, mean (SD)	32.47 (30.64)	44.54 (54.35)	<0.001
Glucose, mean (SD)	4.94 (0.78)	5.23 (1.80)	<0.001
Glycated haemoglobin (HbA1c), mean (SD)	34.66 (4.55)	36.30 (7.24)	<0.001
HDL cholesterol, mean (SD)	1.48 (0.38)	1.37 (0.36)	<0.001
IGF-1, mean (SD)	22.11 (5.31)	20.48 (5.47)	<0.001
LDL direct, mean (SD)	3.58 (0.79)	3.53 (0.85)	0.175
Phosphate, mean (SD)	1.16 (0.15)	1.14 (0.15)	0.004
SHBG, mean (SD)	53.37 (28.23)	47.28 (25.80)	<0.001
Total bilirubin, mean (SD)	9.23 (4.33)	8.08 (3.34)	<0.001
Testosterone, mean (SD)	5.94 (6.00)	5.34 (5.65)	0.022
Total protein, mean (SD)	72.27 (3.75)	71.91 (3.80)	0.031
Triglycerides, mean (SD)	1.62 (0.94)	1.95 (1.20)	<0.001
Urate, mean (SD)	298.19 (75.97)	310.25 (83.09)	<0.001
Vitamin D, mean (SD)	50.16 (20.20)	47.44 (21.40)	0.002

BMI = body mass index; SHBG = sex hormone-binding globulin; IGF-1 = insulin-like growth factor 1; HbA1c = glycated haemoglobin; HDL = high-density lipoprotein; LDL = low-density lipoprotein; SBP = systolic blood pressure; SD = standard deviation. *p*-values are from two-sample *t*-tests for continuous variables and chi-squared tests for categorical variables.

Table 3: Descriptive statistics of covariates stratified by opioid use status among propensity score matched participants with chronic pain in the UK Biobank.

Characteristic	Non-users (n = 518)	Opioid users (n = 518)	p-value
<i>Demographic and lifestyle characteristics</i>			
Sex = male, %	205 (39.6)	217 (41.9)	0.487
Age, mean (SD)	56.27 (7.42)	56.47 (7.53)	0.660
Ethnicity, %			0.388
1 (White)	510 (98.5)	504 (97.3)	
2 (Mixed)	0 (0.0)	3 (0.6)	
3 (Asian or Asian British)	3 (0.6)	6 (1.2)	
4 (Black or Black British)	2 (0.4)	2 (0.4)	
5 (Chinese)	0 (0.0)	1 (0.2)	
6 (Other ethnic group)	3 (0.6)	2 (0.4)	
Education, %			0.979
1 (College or University degree)	176 (34.0)	180 (34.7)	
2 (A levels/AS levels or equivalent)	70 (13.5)	70 (13.5)	
3 (O levels/GCSEs or equivalent)	158 (30.5)	156 (30.1)	
4 (CSEs or equivalent)	37 (7.1)	35 (6.8)	
5 (NVQ or HND or HNC or equivalent)	37 (7.1)	42 (8.1)	
6 (Other professional qualifications eg: nursing, teaching)	40 (7.7)	35 (6.8)	
Smoking status, %			0.838
0 (Never)	265 (51.2)	256 (49.4)	
1 (Previous)	199 (38.4)	208 (40.2)	
2 (Current)	54 (10.4)	54 (10.4)	
Alcohol drinking status, %			0.914
0 (Never)	19 (3.7)	17 (3.3)	
1 (Previous)	28 (5.4)	30 (5.8)	
2 (Current)	471 (90.9)	471 (90.9)	
<i>Anthropometric and socioeconomic measures</i>			
BMI, mean (SD)	29.59 (6.04)	29.51 (5.54)	0.820
Townsend Deprivation Index, mean (SD)	-1.11 (3.07)	-1.13 (2.99)	0.938
<i>Blood biomarkers</i>			
Albumin, mean (SD)	44.94 (2.46)	44.94 (2.43)	0.999
Alkaline phosphatase, mean (SD)	82.47 (22.87)	83.25 (24.36)	0.598
Alanine aminotransferase, mean (SD)	26.05 (18.20)	24.80 (13.54)	0.211
Apolipoprotein A, mean (SD)	1.48 (0.24)	1.49 (0.25)	0.642
Apolipoprotein B, mean (SD)	1.04 (0.23)	1.04 (0.23)	0.927
Aspartate aminotransferase, mean (SD)	27.62 (20.85)	26.12 (9.03)	0.132
Direct bilirubin, mean (SD)	1.56 (0.56)	1.58 (0.59)	0.553
Urea, mean (SD)	5.46 (1.38)	5.46 (1.32)	0.976
Calcium, mean (SD)	2.37 (0.09)	2.37 (0.09)	0.515
Cholesterol, mean (SD)	5.58 (1.03)	5.60 (1.13)	0.800
Creatinine, mean (SD)	70.09 (14.20)	70.90 (14.12)	0.353
C-reactive protein, mean (SD)	3.20 (5.36)	3.37 (4.63)	0.579
Cystatin C, mean (SD)	0.90 (0.14)	0.91 (0.14)	0.146
Gamma glutamyltransferase, mean (SD)	44.70 (59.50)	44.35 (54.48)	0.923
Glucose, mean (SD)	5.16 (1.19)	5.21 (1.77)	0.591
Glycated haemoglobin (HbA1c), mean (SD)	36.15 (6.29)	36.19 (7.08)	0.916
HDL cholesterol, mean (SD)	1.36 (0.35)	1.37 (0.36)	0.601
IGF-1, mean (SD)	20.49 (5.20)	20.52 (5.48)	0.920
LDL direct, mean (SD)	3.53 (0.79)	3.53 (0.85)	0.981
Phosphate, mean (SD)	1.14 (0.15)	1.14 (0.15)	0.836
SHBG, mean (SD)	45.99 (24.52)	47.48 (25.78)	0.341
Total bilirubin, mean (SD)	8.14 (3.17)	8.09 (3.35)	0.815
Testosterone, mean (SD)	5.06 (5.31)	5.35 (5.65)	0.382
Total protein, mean (SD)	71.72 (3.57)	71.88 (3.75)	0.505
Triglycerides, mean (SD)	1.92 (1.04)	1.93 (1.14)	0.812
Urate, mean (SD)	310.32 (81.60)	309.65 (83.17)	0.896
Vitamin D, mean (SD)	47.56 (19.82)	47.63 (21.40)	0.957

BMI = body mass index; SHBG = sex hormone-binding globulin; IGF-1 = insulin-like growth factor 1; HbA1c = glycated haemoglobin; HDL = high-density lipoprotein; LDL = low-density lipoprotein; SBP = systolic blood pressure; DBP = diastolic blood pressure; SD = standard deviation. *p*-values are from two-sample *t*-tests for continuous variables and chi-squared tests for categorical variables.

Table 4: Evaluation of ATE estimators for the effect of opioid use on systolic blood pressure in the UK Biobank chronic pain cohort (testing set).

Method	S-learner				T-learner			
	Bias (Slope)	RMSE	MAE	Cor( $\mathbf{y}, \hat{\epsilon}$ )	Bias (Slope)	RMSE	MAE	Cor( $\mathbf{y}, \hat{\epsilon}$ )
MLR	0.852	20.92	16.19	-0.79	0.853	21.00	16.23	-0.79
UMLR	0.097	55.88	45.10	-0.03	0.096	55.22	44.62	-0.03